Journal of Physics: Conference Series **293** (2011) 012044 doi:10.1088/1742-6596/293/1/012044

The ATLAS Liquid Argon Calorimeter: Overview and Performance

Huaqiao Zhang
on behalf of the ATLAS Liquid Argon Calorimeter Group
CPPM, Aix-Marseille Universite; CNRS/IN2P3, Marseille France
E-mail: huaqiao.zhang@cern.ch

Abstract.
The LHC is delivering collision data since November 2009 up to a 7 TeV center of mass energy world record. The ATLAS experiment has collected more than 1 nb^{-1} collision data until the end of April 2010. The ATLAS Liquid Argon (LAr) calorimeter system, operational since August 2006, has been carefully commissioned and checked using collision data as well as single beam data and cosmic data taken previously. This paper gives an overview of the ATLAS LAr calorimeters status and performance up to the latest 7 TeV collision data. Results on the LAr calorimeters high voltage, LAr temperature, purity and readout electronic stability as well as results on timing alignments and early collision performances are shown here. All indicates that the ATLAS LAr calorimeter system is well commissioned and shows good and promising performances for the physics at LHC era.

1. Introduction

The ATLAS experiment [1] at the Large Hadron Collider (LHC) is a general purpose detector aimed at Higgs and new physics searches as well as precision test of electroweak (EW) mechanisms. It includes an inner tracker, a calorimetry system and a muon spectrometer. The LAr Calorimeters [2], part of the ATLAS calorimetry system, are expected to play leading role in electron, photon, jet and missing E_t measurements and identifications. The test of the LAr calorimeter performances started during the construction. Electron and pion beam tests were performed on prototype and production modules between 1998 and 2004. The LAr calorimeters are operational in the collision cavern since August 2006. In-situ Cosmics data, as well as a short term of beam data in September 2008 and November 2009 were taken before the first LHC collision. Performances were studied and extrapolated to the collisions [3]. ATLAS has collected more than 1 nb^{-1} collision data up to April 2010. This paper reports an overview of the LAr calorimeter system status obtained from years of accumulated data and its in-situ performances from these first collision data.

2. The hardware status of the LAr calorimeters

The LAr calorimeters are sampling calorimeters with liquid argon as active material, full azimuthal angle (ϕ, defined in the transverse x,y plane) coverage and up to [-4.9,4.9] pseudo-rapidity (η) [1] coverage. The LAr calorimeter system includes the electromagnetic barrel

[1] $\eta = -ln(tan(\theta/2))$ where θ is the particle momentum direction versus beam axis polar angle

(EMB) calorimeter ($|\eta| < 1.475$, lead absorber) sitting in the barrel cryostat, and inside an end cap cryostat at each side of the barrel, an electromagnetic end cap (EMEC) calorimeter ($1.375 < |\eta| < 3.2$, lead absorber), a hadronic end cap (HEC) calorimeter ($1.5 < |\eta| < 3.2$, copper absorber), and a forward calorimeter (FCal, $3.1 < |\eta| < 4.9$, copper/tungsten absorber) as shown in Fig. 1. There are three or four longitudinal layers with different granularity in each of them. The EM calorimeter (EMB + EMEC) includes a highly granular accordion layer up to $|\eta| < 2.5$ and a presampler up to $|\eta| < 1.8$, providing information to trigger electron and photon objects (Fig. 2) and ensure proper electron and photon identification and measurement.

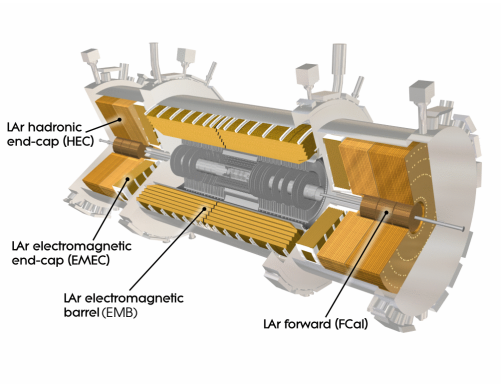

Figure 1. ATLAS LAr calorimeters.

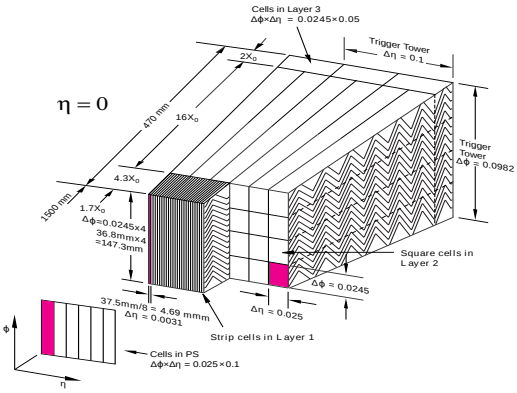

Figure 2. EM calorimeter layers.

The LAr calorimeter system has, in total, 182,468 readout channels/cells, of which 98.6% are operational (4^{th} of May 2010). There are 1.4% dead readout channels, including 20 dead optical transmitters (EMB+EMEC 1.5%, HEC 0.1%, FCal 0%), that will be recovered at a next long shut down. Only 0.0186% electrode channels are unrecoverable.

2.1. High voltage status and liquid argon temperature and purity

High energy particles passing through the LAr calorimeters produce, by interaction with absorbers and LAr, secondary particles traveling in LAr and creating ionized charges. Those charges are drifted by the high voltage (HV) in the liquid argon gap and creates an electric signal on the electrodes. The collected signal depends on the HV and the temperature and purity of the liquid argon.

- HV: LAr calorimeter cells are set to constant HV in $\delta\eta$ x $\delta\phi$ regions of size 0.2*0.2. Only 6% of those HV regions are working at reduced value [4]. Signals in reduced HV regions are recovered with only a small loss of accuracy by correction factors.
- LAr temperature: The LAr signal sensitivity to LAr temperature is -2%/K (density: -0.45%/K , Velocity: -1.55%/K) [5].A homogeneity and stability better than 100 mK is required. The LAr temperature is monitored by probes immersed in the cryostat. The achieved homogeneity, within each cryostat, is 59 mK with 1.5 mK RMS for each probe.
- LAr purity: Gas such as O_2 can capture electrons and reduce signal collection. An impurity level better than 1000 ppb O_2 equivalent is required. Purity monitors [6] in each cryostat show that the impurity level in the LAr is in the range of 200±100 ppb O_2 equivalent.

2.2. LAr calorimeter pulse shape and drift time

Cell collected signals are then amplified, shaped and passed through a switched capacitor array which samples the signal every 25 ns. LAr cells pulse shapes can be predicted from calibration pulses by several models such as Response Transformation Method (RTM) and First Principles Method (FPM). Both model requires that the drift time be measured. Studies of EM calorimeter

drift time use special 32 samplings (25 ns per sampling, 32 samplings covering the full signal pulse region) cosmics runs. The measured drift time is around the expected 460 ns in the barrel and varies with cell gap size in the end cap region. The cosmics results show that the maximum differences of the pulse shape and the predictions are within 2% [7].

2.3. Electronics readout stability

The energy reconstruction of LAr cells is based on an Optimal Filtering algorithm:

$$E_{cell} = F_{\mu A \to MeV}.F_{DAC \to \mu A}.\frac{1}{\frac{M_{phys}}{M_{cali}}}.R.[\sum_{j=1}^{N_{samples}} a_j(s_j - p)], \quad (1)$$

where the pedestals (p), the ramps (R), the Optimal Filtering Coefficients (a_j) and the correction factor for the difference between the calibration and the physics pulse($\frac{1}{\frac{M_{phys}}{M_{cali}}}$) of each cell are monitored by an automatic electronic calibration procedure and stored in a data base that is updated weekly or once significant variations are observed. The calibration run frequency can be up to every LHC fill thus any small deviation of the constants could be corrected within a short time. A study of the calibration constant variations over a six months period shows in Fig. 3 the good stability of the electronic calibration constants. For example, the RMS of EM calorimeter pedestals is less than 0.03 ADC count(typical pedestal is ∼1000 ADC counts).

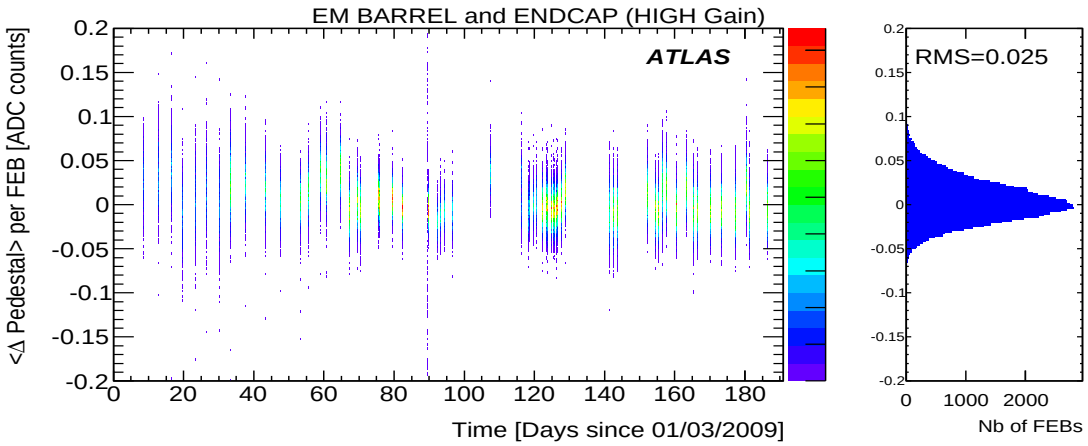

Figure 3. Pedestal stability over six month

2.4. LAr EM calorimeter uniformity measurement with cosmics

Besides the test-beam results, the LAr EM calorimeter response uniformity has also been estimated by comparing cosmics data and MC simulations that did not emulate any non-uniformity. Although this method is limited by muon event properties and statistics (it is hard to extrapolate to electron/photon cases in real collisions), it gives first in-situ uniformity of the ATLAS EM calorimeter. The studies show that the EM barrel second layer non-uniformity is at the level of 1%(as shown in Fig. 4).

3. The LAr calorimeter performances

ATLAS started to record LHC beam data since end of November 2009. These data, first single beam data, then collisions at 900 GeV then at 2.36 TeV and finally at 7 TeV center of mass energy, allowed extensive performance studies of the LAr calorimeter system performances.

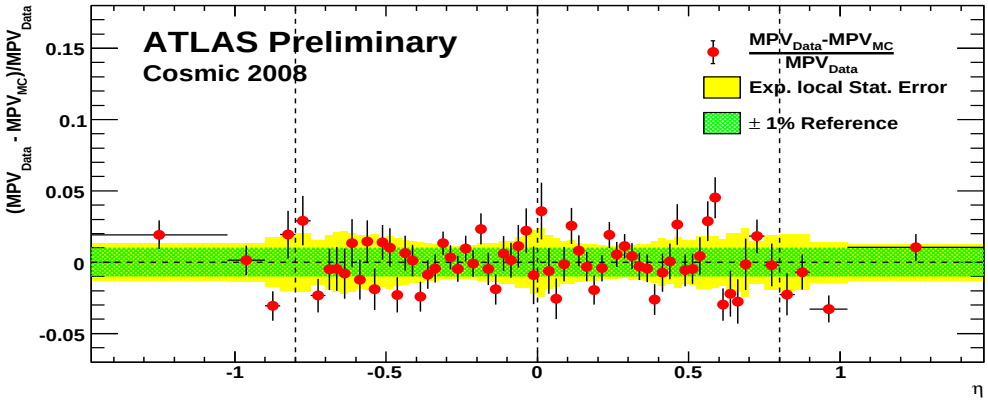

Figure 4. Uniformity of EMB estimated in cosmics data.

3.1. Timing alignment

The so called beam splash events, issued from single beam collisions on a target/collimator 149m far upstream of the ATLAS detector, were used to align timing constants for both the Level one calorimeter trigger and the main LAr calorimeter readout. These events, with both side single beams, created plenty of secondary particles, and fired almost all the ATLAS calorimeters. The LAr Level one (L1Calo) trigger timing constants for all EM trigger towers are now aligned to an accuracy of $\pm$ 5 ns [9]. The LAr calorimeter main readout timing constants were tuned from the average timing of each readout front end board in collision data. An accuracy about 2 ns for all LAr partitions has been achieved for now. With the future increase of collision data statistics, these timing constants will be tuned further at the channel level both for the the L1Calo trigger and the LAr calorimeter systems.

3.2. Level one EM calorimeter trigger performance

The L1Calo trigger and the LAr main readout use the same detector, but different granularity and readout path. An analogue sum is made of all four (or three) layers of LAr EM cells connected to a trigger tower, typically 0.1 x 0.1 in $\delta\eta$ x $\delta\phi$ up to $|\eta| < 2.5$ and grosser trigger tower in higher η region (Fig. 2). The EM L1Calo trigger performance was checked firstly looking at the good correlation of transverse energy (E_T^{L1}) measured by the trigger tower versus the sum E_T^{LAr} of all offline cells connected to this trigger tower as shows in Fig. 5. Then the EM L1Calo trigger E_T resolution with respect to offline sum E_T was measured to be less than 3% at about $E_T > 30GeV$ as shown in Fig. 6, well within the designed 5% E_T resolution. Finally turn on curves of the L1Calo trigger system, such as for the EM5 item, which requires level one EM cluster E_T greater than 5 GeV, have expected performances, as can be seen for EM5 in Fig. 7, and provide electon/photon triggers for offline analysis.

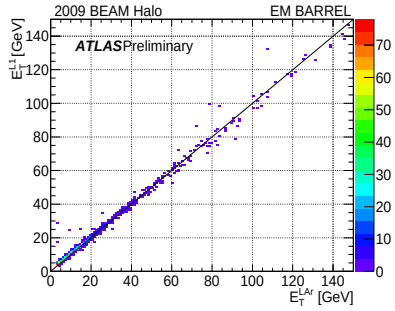

Figure 5. E_T^{L1} versus E_T^{LAr}.

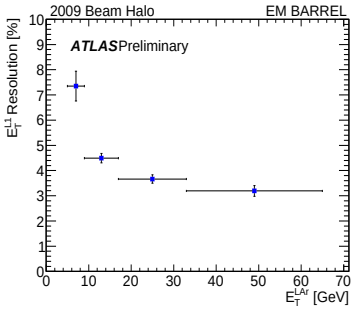

Figure 6. E_T^{L1} resolution versus E_T^{LAr}.

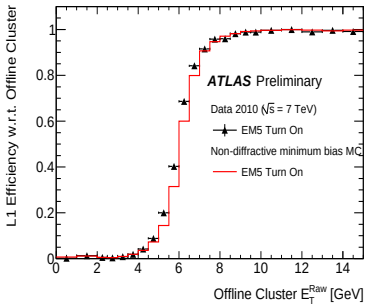

Figure 7. EM5 L1CALO Trigger Turn on.

3.3. LAr noise and missing transverse energy in random events

Fig. 8 shows the noise measured with random trigger events at the cell level as a function of η for all LAr layers. It is in agreement with expectations. The noise of single cells is constantly checked by the online monitoring system. The noise can also be checked through global cell quantities such as missing transverse energy E_T^{miss} in random events. The definition is:

$$E_T^{\text{miss}} = \sqrt{(\sum E_x^{\text{miss}})^2 + (\sum E_y^{\text{miss}})^2} \tag{2}$$

Summing up all the LAr cells above two sigma of noise, the obtained LAr calorimeters E_T^{miss} agrees well with the gaussian model. However, as shown in Fig. 9, better noise suppression is achieved with a dynamical topological cluster summed E_T^{miss}, which is used as the default physics E_T^{miss} algorithm.

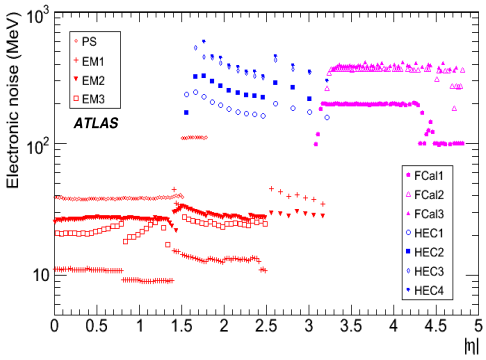

Figure 8. LAr noise at cell level

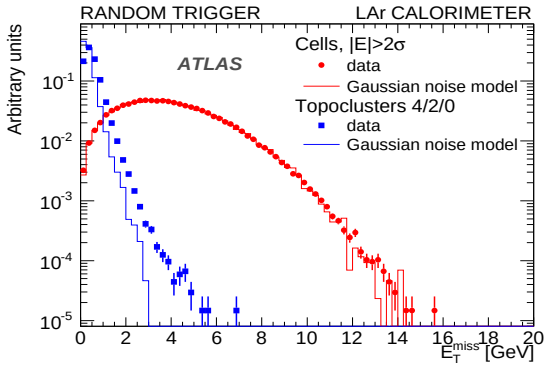

Figure 9. E_T^{miss} in random events

3.4. LAr calorimeter energy flow

The energy deposited in LAr cells by collision data is compared to Non-Diffractive minimum bias Monte Carlo simulations and to random trigger events. The collision signal tails is well visible in all LAr calorimeters and the simulation agrees well with the data as shown for the endcap electromagntic calorimeter in Fig. 10. A more detailed check of LAr calorimeter energy flow is done by looking at the occupancy map of each calorimeter layer. This map is obtained for each layer by summing up, for all selected minimum bias 7 TeV events, all the cells with energy above $5\sigma_{\text{noise}}$. The occupancy convolutes physics and detector performance problems. Each hot/cold zone in the map shown in Fig. 11 is identified as detector defects, such as for example the blank areas which are dead readout regions or the green squares which are non nominal HV regions, and have been taken care off.

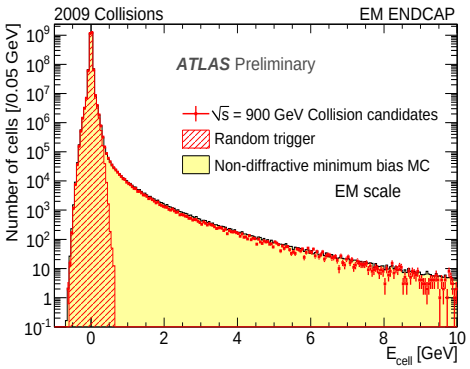

Figure 10. Cell energy distribution

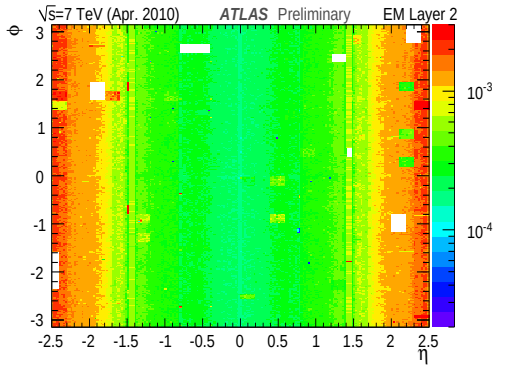

Figure 11. EM calorimeter occupancy.

3.5. Electron, photon, jet, E_T^{miss}

After the check of the LAr calorimeters global performances, the study of electrons, photons, jets and E_T^{miss} [10] has been made with the first 900 GeV and 7 TeV collision data. As an example, the E_T^{miss} distribution from a topological cluster algorithm is shown in Fig. 14. The di-jet $\delta\phi$ distribution from Anti-k_t jet algorithm is shown in Fig. 13. And after a careful selection of photon candidates, a reconstructed invariant $\gamma\gamma$ mass spectrum is produced, as shown in Fig. 12, with visible π^0 and η^0 signal peaks. For all of those distributions, the agreement between the simulation and the data is good at 900 GeV as well as at 7 TeV, illustrating the excellent performances of the LAr calorimeter system.

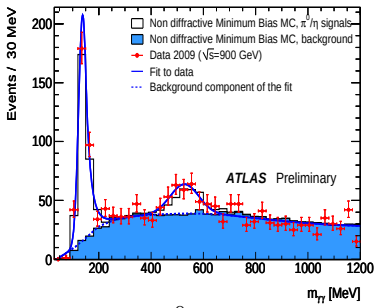

Figure 12. π^0 and η signal

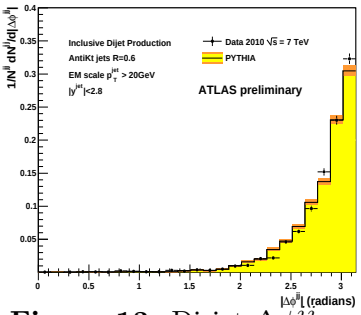

Figure 13. Di-jet $\Delta\phi^{jj}$.

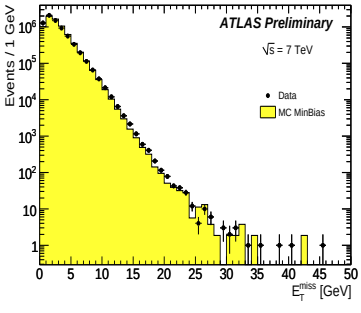

Figure 14. Missing E_t.

4. Conclusion

The studies of recent collision data as well as years of test-beam, cosmics and single beam data recorded by the ATLAS detector, assess the excellent performance of the Liquid Argon Calorimeters. Remarkable stability of the LAr temperature, purity, and electronics is achieved well within the designed requirements. Less than 1% overall energy response non-uniformity even in the cosmics data, $\pm$ 2 ns overall LAr timing in the first collision data and a well modeled and monitored noise. The first performance measurements of the LAr trigger system, that's to say electron, photon, jet and E_T^{miss} reconstruction using collision data show very promising results and allow the first observation of particle peaks, such as π^0 and η^0. The LAr calorimeter system is now ready for the long ongoing data campaign.

References

[1] G Aad et al, The ATLAS Experiment at the CERN Large Hadron Collider, The ATLAS Collaboration `JINST 3` (2008) S08003
[2] ATLAS liquid argon calorimeter: Technical design report, The ATLAS Collaboration, CERN-LHCC-96-41 (1996)
[3] G.Aad et al., Readiness of the ATLAS Liquid Argon Calorimeter for LHC Collisions, The ATLAS Collaboration, Accepted by EPJC
[4] B.Belhorma et al., Evaporating short-circuits in the ATLAS liquid argon barrel presampler, ATL-LARG-PUB-2005-003
[5] C. de la Taille, Temperature dependence of the ATLAS electromagnetic calorimeter signal. Preliminary drift time measurement. ATL-LARG-95-029 (1995)
[6] M.Adams et al., A purity monitoring system for liquid argon calorimeters, Nucl. Inst.Meth. A 545 (2000) 613-623
[7] G.Aad et al., Drift Time Measurement in the ATLAS Liquid Argon Electromagnetic Calorimeter using Cosmic Muons, The ATLAS Collaboration, Accepted by EPJC
[8] H. Abreu et al., Performance of the Electronic Readout of the ATLAS Liquid Argon Calorimeters, Accepted by JINST
[9] ATLAS Level-1 Calorimeter Trigger: Timing Calibration with 2009 LHC Beam Splashes, The ATLAS Collaboration, ATL-DAQ-PUB-2010-001
[10] The ATLAS collaboration, ATLAS-CONF-2010-001, ATLAS-CONF-2010-005, ATLAS-CONF-2010-006, ATLAS-CONF-2010-008